Prospective Phase II Trial of [^{68}Ga]Ga-NODAGA-E[c(RGDyK)]$_2$ PET/CT Imaging of Integrin $\alpha_v\beta_3$ for Prognostication in Patients with Neuroendocrine Neoplasms

Esben Andreas Carlsen[1,2], Mathias Loft[1,2], Annika Loft[1,2], Dorota Czyzewska[1,2], Mikkel Andreassen[2,3], Seppo W. Langer[2,4,5], Ulrich Knigge[2,3,6], and Andreas Kjaer[1,2]

[1]Department of Clinical Physiology and Nuclear Medicine & Cluster for Molecular Imaging, Copenhagen University Hospital, Rigshospitalet & Department of Biomedical Sciences, University of Copenhagen, Copenhagen, Denmark; [2]ENETS Neuroendocrine Tumor Center of Excellence, Copenhagen University Hospital, Rigshospitalet, Copenhagen, Denmark; [3]Department of Clinical Endocrinology, Copenhagen University Hospital, Rigshospitalet, Copenhagen, Denmark; [4]Department of Oncology, Copenhagen University Hospital, Rigshospitalet, Copenhagen, Denmark; [5]Department Clinical Medicine, University of Copenhagen, Copenhagen, Denmark; and [6]Department of Surgical Gastroenterology, Copenhagen University Hospital, Rigshospitalet, Copenhagen, Denmark

Integrin $\alpha_v\beta_3$, a subtype of the arginine-glycine-aspartate (RGD)–recognizing cell surface integrins, is upregulated on endothelial cells during angiogenesis and on tumor cells. Because of involvement in tumor growth, invasiveness and metastases, and angiogenesis, integrin $\alpha_v\beta_3$ is an attractive target in cancers. In this study, we applied ^{68}Ga-NODAGA-E[c(RGDyK)]$_2$ for imaging of integrin $\alpha_v\beta_3$ in patients with neuroendocrine neoplasms (NENs) and its potential use for prognostication. We hypothesized that ^{68}Ga-NODAGA-E[c(RGDyK)]$_2$ PET/CT would show tumor lesion uptake and that higher tumor lesion uptake was associated with a poorer prognosis. **Methods:** Between December 2017 and November 2020 we prospectively enrolled 113 patients with NEN of all grades (2019 World Health Organization classification) for ^{68}Ga-NODAGA-E[c(RGDyK)]$_2$ PET/CT. The scan was acquired 45 min after injection of 200 MBq of ^{68}Ga-NODAGA-E[c(RGDyK)]$_2$. Board-certified specialists in nuclear medicine and radiology analyzed the PET/CT measuring SUV_{max} in tumor lesions. Positive tumor lesions were defined as those with tumor-to-liver background ≥ 2. Maximal tumor SUV_{max} for each patient was used as a predictor of outcome. Patients were followed for at least 1 y to assess progression-free survival and overall survival. **Results:** Of 113 patients enrolled in the trial, 99 underwent ^{68}Ga-NODAGA-E[c(RGDyK)]$_2$ PET/CT, with 97 patients having evaluable lesions. The patients predominantly had small intestinal (64%) or pancreatic (20%) NEN and most had metastatic disease (93%). Most patients had low-grade tumors (78%), whereas 22% had high-grade tumors. During a median follow-up of 31 mo (interquartile range, 26–38 mo), 62 patients (64%) experienced disease progression and 25 (26%) patients died. In total, 76% of patients had positive tumor lesions, and of the patients with high-grade tumors 91% had positive tumor lesions. High integrin $\alpha_v\beta_3$ expression, defined as an SUV_{max} of at least 5.25, had a hazard ratio of 2.11 (95% CI, 1.18–3.78) and 6.95 (95% CI, 1.64–29.51) for progression-free survival and overall survival, respectively ($P = 0.01$ for both). **Conclusion:** Tumor lesion uptake of ^{68}Ga-NODAGA-E[c(RGDyK)]$_2$ was evident in patients with all grades of NEN. High uptake was associated with a poorer prognosis. Further studies are warranted to establish whether ^{68}Ga-NODAGA-E[c(RGDyK)]$_2$ PET/CT may become a prediction tool for identification of patients eligible for treatments targeting integrin $\alpha_v\beta_3$.

Key Words: integrin $\alpha_v\beta_3$; neuroendocrine neoplasms; PET; prognosis; molecular imaging

J Nucl Med 2023; 64:252–259
DOI: 10.2967/jnumed.122.264383

Neuroendocrine neoplasms (NENs) represent a heterogeneous group of tumors originating from the neuroendocrine cells. NEN are primarily found in the gastrointestinal tract, pancreas, and lungs. Patients with NEN are often diagnosed when the disease has metastasized, yet the clinical course for these patients varies greatly. Origin of primary tumor, presence of metastases as well as tumor morphology and proliferation activity (i.e., Ki-67) are known prognostic factors (*1*). The 2019 World Health Organization (WHO) classification stratifies NEN into neuroendocrine tumor (NET) G1 (Ki-67 < 3%), NET G2 (Ki-67 3%–20%), NET G3 (Ki-67 > 20% and well-differentiated), and neuroendocrine carcinoma (NEC) (Ki-67 > 20% and poorly differentiated) (*2*). Furthermore, imaging modalities aid in diagnosis, staging, treatment selection, and follow-up for patients with NEN. In particular, PET radiotracers reflecting somatostatin receptor expression (e.g., ^{64}Cu-DOTATATE or ^{68}Ga-DOTATATE) and glucose metabolism (^{18}F-FDG) are used for these purposes in addition to providing prognostic information (*3,4*). Finally, targeting the somatostatin receptors with peptide receptor radionuclide therapy (PRRT), for example, ^{177}Lu-DOTATATE, has been approved for patients with NEN.

Additional tumor markers may be useful for further improvement in prognostication and ultimately identifying novel treatment targets in patients with NEN. Cell surface adhesion receptors of the integrin superfamily have been extensively investigated because their role in physiologic as well as in pathophysiologic processes, and especially in cancers (*5*). The subfamily of arginine-glycine-aspartate (RGD)–recognizing integrins has implications on several of hallmarks of cancer: tumor growth, invasiveness, and metastases and angiogenesis. Integrin $\alpha_v\beta_3$ is significantly upregulated on activated endothelial cells during angiogenesis but absent on quiescent endothelial cells as well as overexpressed on tumor cells in several cancers (*6*). NENs are generally characterized as highly vascularized tumors with overexpression of various proangiogenetic factors such as vascular endothelial growth factor (*7*). Previously we found, using quantitative gene expression,

Received May 20, 2022; revision accepted Aug. 13, 2022.
For correspondence or reprints, contact Andreas Kjaer (akjaer@sund.ku.dk).
Published online Aug. 18, 2022.

that the expression of integrin $\alpha_v\beta_3$ shows high variability between NENs (*8*). Because of its integral role in cancer, our group therefore developed and clinically translated the PET radiotracer ^{68}Ga-NODAGA-E[c(RGDyK)]$_2$ targeting integrin $\alpha_v\beta_3$ with high affinity (*9,10*).

The aim of this phase II clinical trial of ^{68}Ga-NODAGA-E[c(RGDyK)]$_2$ PET/CT in patients with NEN of all grades was to further assess tumor uptake and prognostic value. We hypothesized that PET/CT with ^{68}Ga-NODAGA-E[c(RGDyK)]$_2$ would show accumulation in tumor lesions in patients with NEN of all grades and that the uptake of the radiotracer would be associated with progression-free survival (PFS) and overall survival (OS).

MATERIALS AND METHODS

Patients

Patients with histologically confirmed NEN were included from the Department of Endocrinology (managing low-grade NEN, Ki-67 $\leq$ 20%) and Department of Oncology (managing high-grade NEN, Ki-67 $>$ 20%), Copenhagen University Hospital–Rigshospitalet, Denmark, between December 4, 2017, and November 26, 2020. Rigshospitalet is a Neuroendocrine Tumor Center of Excellence accredited by the European Neuroendocrine Tumor Society. The study was conducted in accordance with the Helsinki Declaration and Good Clinical Practice. The study was approved by the Danish Medicines Agency (EudraCT 2017-002512-14), Scientific Ethics Committee (H-17019542), and Danish Data Protection Agency (2012-58-0004), and registered on clinicaltrials.gov (NCT03271281).

Eligible patients were 18 y or older, capable of reading and understanding the patient information in Danish and giving informed consent, diagnosed with gastroenteropancreatic NEN of all grades or bronchopulmonary NEN, and had a WHO performance status of 0–2. Patients were excluded if they were pregnant or breastfeeding, had a body mass more than 140 kg, or had a history of allergic reaction attributable to compounds of chemical or biologic composition similar to ^{68}Ga-NODAGA-E[c(RGDyK)]$_2$ or in the case of bronchopulmonary NEN if the subtype was small cell lung cancer. After written informed consent was obtained, the patients were referred for a ^{68}Ga-NODAGA-E[c(RGDyK)]$_2$ PET/CT at the first opportunity.

Image Acquisition

Data were acquired using a Biograph 128 mCT PET/CT scanner (Siemens Medical Solutions) with an axial field of view of 216 mm. On the basis of the previous phase I trial, the scans were acquired 45 min after intravenous administration of approximately 200 MBq of ^{68}Ga-NODAGA-E[c(RGDyK)]$_2$ ([^{68}Ga]Ga-NODAGA-Glu[cyclo(-Arg-Gly-Asp-D-Tyr-Lys-)]$_2$) equaling 4.4 mSv. Radiotracer were produced as previously described (*9*). Whole-body PET scans (mid orbita to mid thigh) were obtained with an acquisition time of 4 min per bed position. Attenuation- and scatter-corrected PET data were reconstructed iteratively using a 3-dimensional ordinary Poisson ordered-subset expectation maximization algorithm including point-spread function and time-of-flight information using the TrueX algorithm (Siemens Medical Solutions); the settings were 2 iterations, 21 subsets, 2-mm gaussian filter. A diagnostic CT scan was obtained before the PET scan with a 2-mm slice thickness, 120 kV, and a quality reference of 225 mAs modulated by the Care Dose 4D automatic exposure control system (Siemens Medical Solutions). An automatic injection system was used to administer 75 mL of an iodine-containing contrast agent (Optiray 300; Covidien) for arterial and venous phase CT.

Patients were observed for adverse events after injection of ^{68}Ga-NODAGA-E[c(RGDyK)]$_2$, and after discharge patients were asked to

TABLE 1
Baseline Characteristics of 97 Patients with NENs

Baseline characteristic	Data
Median age (y)	67 (range, 44–83)
Sex	
Female	43 (44%)
Male	54 (56%)
Site of primary tumor	
Small intestine	62 (64%)
Pancreas	19 (20%)
Lung	6 (6%)
Colon	6 (6%)
Stomach	2 (2%)
Esophagus	1 (1%)
Rectum	1 (1%)
Metastatic disease	90 (93%)
Liver metastases	76 (79%)
Median Ki-67 (%)	6 (range, 1–100)
2019 World Health Organization grade	
NET G1	21 (22%)
NET G2	55 (57%)
NET G3	14 (14%)
NEC	7 (7%)
Median time from diagnosis to PET/CT (mo)	27 (range, 2–265)
Primary tumor resected	37 (38%)
Ongoing treatment at PET/CT scan time	
Somatostatin analog	75 (77%)
Interferon	8 (8%)
Capecitabine/5-fluorouracil	5 (5%)
Etoposide ± carboplatin	4 (4%)
Streptozotocin	4 (4%)
Everolimus	3 (3%)
Temozolomide	2 (2%)
Completed treatment before PET/CT	
On first line of therapy	45 (46%)
Peptide receptor radionuclide therapy	30 (31%)
Etoposide ± carboplatin	16 (16%)
Capecitabine/5-fluorouracil	12 (12%)
Temozolomide	7 (7%)
Streptozotocin	7 (7%)
Interferon	6 (6%)
External radiation therapy	5 (5%)
Liver radiofrequency ablation or embolization	5 (5%)
Resection of liver metastases	4 (4%)
Everolimus or sunitinib	2 (2%)

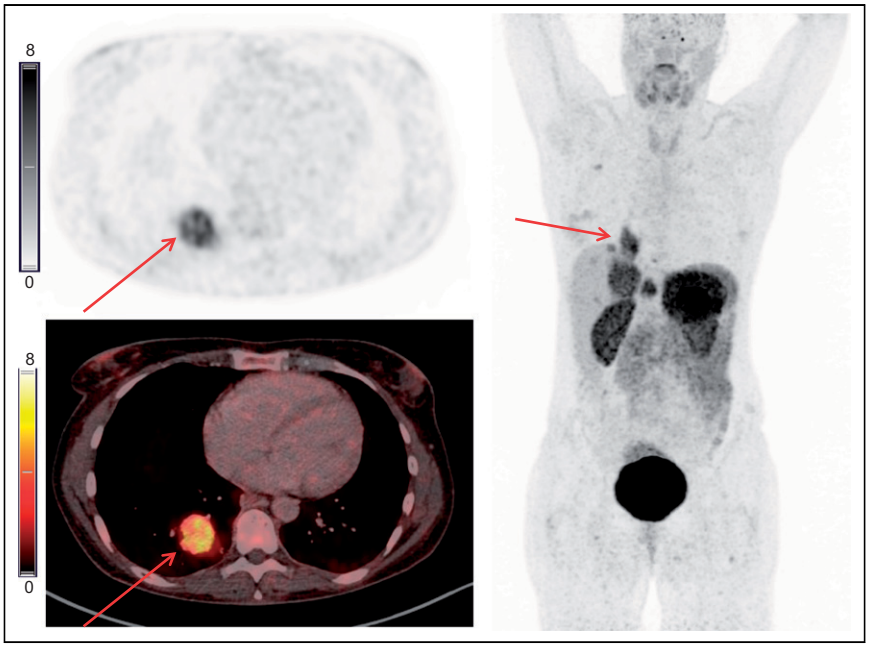

FIGURE 1. Example of ^{68}Ga-NODAGA-E[c(RGDyK)]$_2$ PET/CT. Transaxial PET and fused PET/CT and maximum-intensity projection with color bars (unit: SUV). Patient with lung NET grade 2 (Ki-67 15%) with liver and bone metastases. Arrows point to primary tumor.

record any adverse events occurring within the first 24 h of injection. Adverse events were categorized according to Common Terminology Criteria for Adverse Events (version 5.0).

Image Analysis

Together, an experienced board-certified nuclear medicine physician and an experienced board-certified radiologist analyzed the ^{68}Ga-NODAGA-E[c(RGDyK)]$_2$ PET/CT scans. The readers had access to previous imaging studies but were masked to other patient data and follow-up data. Lesions were identified on CT or PET. SUV was calculated as decay-corrected measured radioactivity concentration/(injected activity/body weight). If more than 1 lesion was present in an organ, the lesion with the highest SUV_{max} was noted. If no lesions were identified on PET, but lesions were visible on CT, the largest lesion (based on viable tissue within the lesion) on CT was used as guide for lesion delineation on the PET scan from which SUV_{max} was determined. As background reference of uptake in tumor lesions, the radiotracer uptake in normal liver tissue was measured as SUV_{mean}. A tumor lesion–to–liver ratio (TLR) was calculated as tumor lesion SUV_{max}/normal liver SUV_{mean}. A cutoff of TLR $\geq$ 2 was used to define positive lesions.

Follow-up

The patients were followed at the Rigshospitalet Neuroendocrine Tumor Center of Excellence with regular visits including clinical examination, blood samples, and imaging (CT, MR, ultrasound, or PET/CT). The frequency was in accordance with European Neuroendocrine Tumor Society guidelines, typically every 3–6 mo (*11*). The ^{68}Ga-NODAGA-E[c(RGDyK)]$_2$ PET/CT was not made available for the treating physicians and thus not used to guide clinical decisions regarding treatment or follow-up. The end of follow-up was December 31, 2021, for the current study. Routine CT and or MRI were used for evaluation of PFS in accordance with RECIST (version 1.1) (*12*). PFS was defined as time from ^{68}Ga-NODAGA-E[c(RGDyK)]$_2$ PET/CT to, if any, progression or death from any cause. If no progression or death from any cause occurred within the follow-up time period, the patient was censored at the time of last available diagnostic imaging. OS was defined as time from ^{68}Ga-NODAGA-E[c(RGDyK)]$_2$ PET/CT to death by any cause. As all deaths but 2 were directly related to NEN, we refrained from analyzing disease-specific survival. Patients alive at follow-up were censored to the day of the end of follow-up (December 31, 2021).

Statistics

Continuous variables are reported as mean ± SD or median with range unless otherwise noted. Kaplan–Meier analyses were used for estimation of time to outcome (PFS and OS) and reverse Kaplan–Meier analysis was used to estimate median follow-up time. Univariate and multivariate Cox regression analyses for OS and PFS, with predictor variables being SUV_{max} and WHO grade, were performed to determine hazard ratio (HR) and 95% CI. We used the Cutoff Finder application to determine the optimal cutoff for SUV_{max} (*13*). A P value of less than 0.05 was considered statistically significant. R version 3.6.0 (R Foundation for Statistical Computing) was used for the analyses.

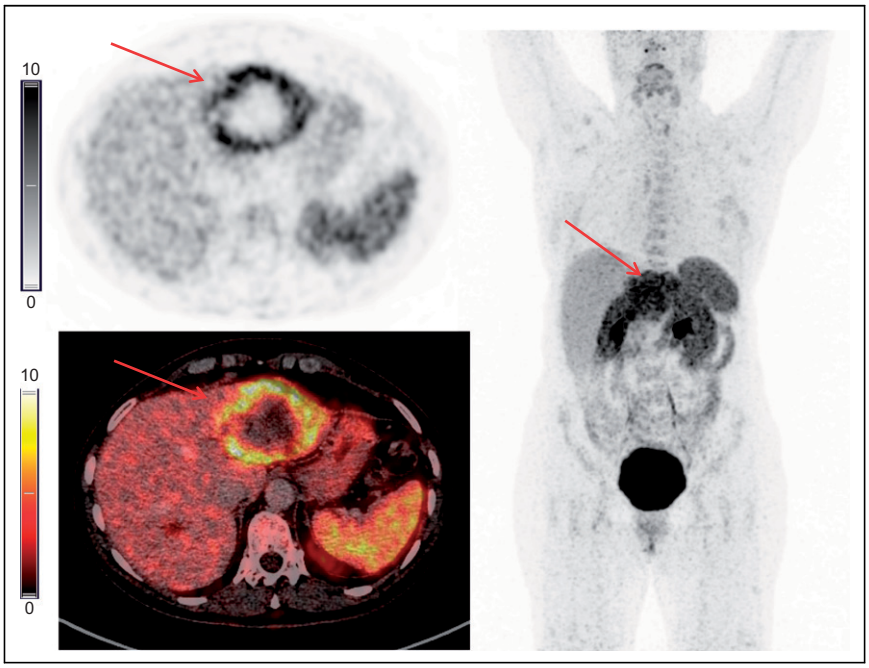

FIGURE 2. Example of ^{68}Ga-NODAGA-E[c(RGDyK)]$_2$ PET/CT. Transaxial PET and fused PET/CT and maximum-intensity projection with color bars (unit: SUV). Patient with gastric NET grade 2 (Ki-67 8%) with liver metastases. Arrows point to liver metastasis.

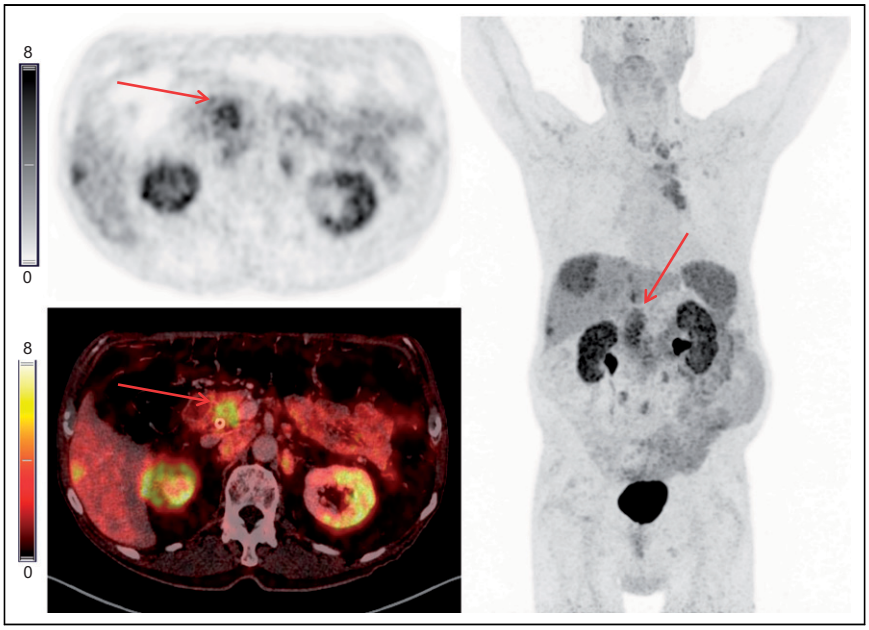

FIGURE 3. Example of ^{68}Ga-NODAGA-E[c(RGDyK)]$_2$ PET/CT. Transaxial PET and fused PET/CT and maximum-intensity projection with color bars (unit: SUV). Patient with pancreatic NET grade 2 (Ki-67 11%) with liver and lymph node metastases. Arrows point to primary tumor.

RESULTS

Patients and Image Acquisition

We prospectively included 113 patients, 14 of whom did not undergo ^{68}Ga-NODAGA-E[c(RGDyK)]$_2$ PET/CT because of disease worsening (n = 4), consent withdrawal (n = 2), death before PET/CT (n = 3), logistical impossibility for PET/CT to be performed (n = 2), and infeasibility for PET/CT scanning due to COVID-19 restrictions (n = 3). Of the 99 patients scanned with PET/CT, 97 patients had evaluable lesions. The patients predominately had small intestinal (n = 62, 64%) or pancreatic (n = 19, 20%) NEN and metastatic disease (n = 90, 93%) (Table 1). Most patients had low-grade tumors (Ki-67 ≤ 20%) (n = 76, 78%), whereas 21 (22%) had high-grade tumors (Ki-67 > 20%). No patients were treatment-naïve before the PET/CT scan.

Patients undergoing ^{68}Ga-NODAGA-E[c(RGDyK)]$_2$ PET/CT (n = 99) received a median mass dose of 18.9 (range, 7.7–49.3) μg of ^{68}Ga-NODAGA-E[c(RGDyK)]$_2$ and the activity dose was 193 (range, 104–226) MBq. Median time from injection to the start of PET scanning was 47 min (range, 35–86 min). Three patients experienced an adverse event: dizziness (grade 1), fall (grade 1), and infusion-related reaction to injection of CT contrast (grade 2) within 24 h of injection of ^{68}Ga-NODAGA-E[c(RGDyK)]$_2$. All were deemed unrelated to ^{68}Ga-NODAGA-E[c(RGDyK)]$_2$ injection. No grade 3–5 adverse events occurred.

TABLE 2
Patients with ^{68}Ga-NODAGA-E[c(RGDyK)]$_2$ PET–Positive Lesions (TLR ≥ 2) According to WHO Classification of NENs

Uptake ratio	NET G1 (n = 21)	NET G2 (n = 55)	NET G3/NEC (n = 21)	All (n = 97)
TLR ≥ 2	13 (62%)	42 (76%)	19 (91%)	74 (76%)
TLR < 2	8 (38%)	13 (24%)	2 (10%)	23 (24%)

A tumor was defined as positive when the TLR, measured as lesion SUV_{max}–to–normal liver SUV_{mean}, was ≥ 2. Of the patients with NET G3/NEC tumors, 13 of 14 (93%) patients with NET G3 were positive and 6 of 7 (86%) patients with NEC were positive.

TABLE 3
Treatments Given to Patients with NENs (n = 97) During Follow-up

Treatment after PET/CT	n (%)
Somatostatin analog	78 (80%)
Peptide receptor radionuclide therapy	31 (32%)
Capecitabine/5-fluorouracil	13 (13%)
Everolimus or sunitinib	12 (12%)
Surgery	11 (11%)
Temozolomide	9 (9%)
Liver radiofrequency ablation or embolization	9 (9%)
External radiation therapy	7 (7%)
Etoposide ± carboplatin	5 (5%)
Interferon	5 (5%)
Streptozotocin	3 (3%)
Docetaxel	3 (3%)

Image Analysis

The median maximal tumor lesion SUV_{max} was 6.1 (range, 1.4–14.1). The mean ± SD of tumor lesion SUV_{max} was 6.36 ± 2.49 and the mean ± SD normal liver SUV_{mean} was 2.41 ± 0.55. Examples of ^{68}Ga-NODAGA-E[c(RGDyK)]$_2$ PET/CT are shown in Figures 1–3. When the cutoff of TLR ≥ 2 to determine positive lesions was applied, approximately two thirds of patients with NET G1 had positive lesions, which gradually increased to nearly all patients with NET G3/NEC (91%) having positive lesions (Table 2). In total, 76% of patients had positive tumor lesions.

Follow-up

During a median follow-up of 31 mo (interquartile range, 26–38 mo), 62 patients (64%) experienced disease progression and 25 (26%)

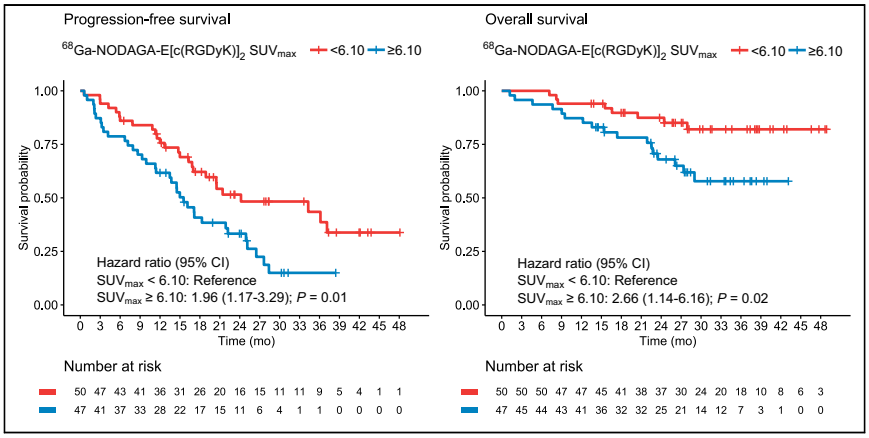

FIGURE 4. Kaplan–Meier plots of ^{68}Ga-NODAGA-E[c(RGDyK)]$_2$ PET SUV_{max} dichotomized at 6.10 (median) for prediction of PFS and OS.

in Table 3. Treatment with somatostatin analog was the most frequent (80%, 78/97), and 32% (31/97) of all patients underwent PRRT during the follow-up period.

PFS and OS

In univariate analyses, the maximal tumor SUV_{max} as a continuous variable was significantly associated with PFS and OS, with an HR of 1.17 (95% CI, 1.07–1.28), $P < 0.001$, and 1.19 (95% CI, 1.03–1.38), $P = 0.02$, per 1 unit increase, respectively. High integrin $\alpha_v\beta_3$ expression, defined as maximal tumor SUV_{max} above median (SUV_{max} 6.10) had an HR of 1.96 (95% CI, 1.17–3.29) and 2.66 (95% CI, 1.14–6.16) for PFS and OS, respectively ($P < 0.05$ for

TABLE 4
Uni- and Multivariate Cox Regression Analyses for PFS (SUV_{max} Cutoff at 6.10)

	Univariate Cox		Multivariate Cox	
PFS	HR	*P*	HR	*P*
SUV_{max}				
<6.10	Reference	—	Reference	—
≥6.10	1.96 (1.17–3.29)	0.01	1.82 (1.07–3.08)	0.03
WHO grades				
NET G1	Reference		Reference	
NET G2	1.25 (0.63–2.49)	0.52	1.25 (0.63–2.49)	0.52
NET G3	4.01 (1.68–9.54)	<0.01	4.08 (1.70–9.77)	<0.01
NEC	7.01 (2.65–18.50)	<0.001	5.87 (2.21–15.61)	<0.001

The median SUV_{max} was 6.10. Data in parentheses are 95% CIs.

patients died. Overall median PFS was 18.9 mo (interquartile range, 15.5–25.1 mo). No patients were lost to follow-up. The patients' treatments after ^{68}Ga-NODAGA-E[c(RGDyK)]$_2$ PET/CT are given both (Fig. 4; Tables 4 and 5). Optimal cutoffs for dichotomizing maximal tumor SUV_{max} were assessed by Cutoff Finder for either PFS or OS as outcome (Supplemental Fig. 1; supplemental materials

TABLE 5
Uni- and Multivariate Cox Regression Analyses for OS (SUV_{max} Cutoff at 6.10)

	Univariate Cox		Multivariate Cox	
OS	HR	*P*	HR	*P*
SUV_{max}				
<6.10	Reference	—	Reference	—
≥6.10	2.66 (1.14–6.16)	0.02	2.59 (1.08–6.24)	0.03
WHO grades				
NET G1	Reference		Reference	
NET G2	1.84 (0.40–8.50)	0.44	1.80 (0.39–8.35)	0.45
NET G3	15.99 (3.26–78.50)	<0.01	18.04 (3.59–90.63)	<0.001
NEC	28.46 (5.62–144.24)	<0.001	22.55 (4.45–114.27)	<0.001

The median SUV_{max} was 6.10. Data in parentheses are 95% CIs.

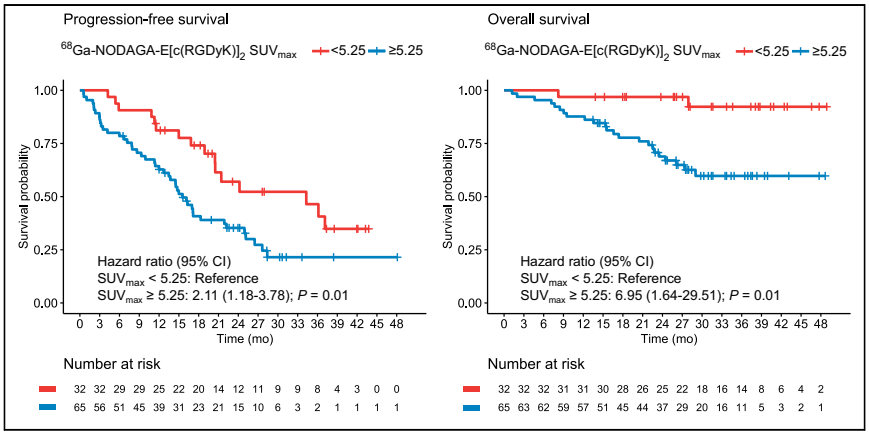

FIGURE 5. Kaplan–Meier plots of ^{68}Ga-NODAGA-E[c(RGDyK)]$_2$ PET SUV_{max} dichotomized at 5.25 for prediction of PFS and OS.

are available at http://jnm.snmjournals.org). When a lower cutoff of SUV_{max} (5.25) was used, a smaller group of patients (n = 32) with a very low risk of death could be identified (Fig. 5; Tables 6 and 7). Patients with an SUV_{max} above 5.25 had an HR of 2.11 (95% CI, 1.18–3.78) and 6.95 (95% CI, 1.64–29.51) for PFS and OS, respectively (P = 0.01 for both). With the cutoff of 5.25, median OS was not reached in either groups with low or groups with high SUV_{max}, and median PFS was 34.3 mo (20.5; upper limit not reached) for patients with low SUV_{max} versus 15.5 mo (13.5–22.2) for patients with high SUV_{max}. Furthermore, when a higher cutoff of SUV_{max} of 7.45 was used, the dichotomization was optimized for prediction of disease progression with an HR of 2.57 (95% CI, 1.52–4.34), $P <$ 0.001 (Supplemental Fig. 2; Supplemental Tables 1 and 2). Patients with NET G3 and NEC had significantly worse PFS and OS as compared with patients with NET G1, whereas no difference was seen between NET G2 and NET G1 (Tables 4 and 5). In multivariate analyses including SUV_{max} and WHO classification (NET G3 and NEC vs. NET G1), both remained significantly associated with PFS and OS (Tables 4–7).

DISCUSSION

The major finding of our phase II prospective study of ^{68}Ga-NODAGA-E[c(RGDyK)]$_2$ PET/CT for integrin $\alpha_v\beta_3$ imaging in patients with NEN was that integrin $\alpha_v\beta_3$ expression was seen in both low- and high-grade NEN. Furthermore, we found a significant association between radiotracer uptake and both PFS and OS. When dichotomized at SUV_{max} 5.25, patients with higher radiotracer uptake in tumor lesion had a 2-fold higher risk of progressive disease and a 7-fold higher risk of death. These findings highlight integrin $\alpha_v\beta_3$ as an important prognostic marker in patients with NEN.

Many radiotracers using the RGD motif have been tested preclinically, with only some being further translated into clinical trials (*14*). In our phase I trial on ^{68}Ga-NODAGA-E[c(RGDyK)]$_2$ PET/CT imaging, we included patients with NEN or breast cancer and demonstrated that administration of the radiotracer was safe and had low radiation burden and high tumor lesion uptake (*9*). Besides our phase I trial, no specific PET imaging studies with an RGD-based radiotracer in patients with NEN have been conducted, although combined integrin $\alpha_v\beta_3$ and somatostatin receptor targeting has been examined with ^{68}Ga-NOTA-3P-TATE-RGD PET/CT (*15*). To our knowledge, the current study is the largest to be conducted with an RGD-based PET radiotracer. Other clinical trials have used RGD-based radiotracers to examine patients with, for example, breast cancer and head and neck cancers, as well as several other nononcologic applications, for example, atherosclerosis and rheumatoid arthritis (*16–19*).

Integrin $\alpha_v\beta_3$ is a cell surface adhesion receptor and a member of the integrin superfamily. The subfamily of integrins recognized by RGD also includes $\alpha_v\beta_1$, $\alpha_v\beta_5$, $\alpha_v\beta_6$, $\alpha_v\beta_8$, $\alpha_5\beta_1$, $\alpha_8\beta_1$, and $\alpha_{IIb}\beta_3$ (*20*). Integrins are involved in several physiologic and pathophysiologic pathways, for example, embryogenesis, wound healing, and angiogenesis as well as tumor growth, invasion or metastasis, and angiogenesis related to cancer. The natural ligands of integrin $\alpha_v\beta_3$ are extracellular matrix proteins such as fibronectin and vitronectin. Additionally, integrins interact with several other factors also involved in angiogenesis and invasive growth, for example, vascular endothelial growth factor and urokinase plasminogen activator receptor (*5,21*). An indication that integrin expression is involved in promoting the metastatic process in patients with NEN is supported by

TABLE 6
Uni- and Multivariate Cox Regression Analyses for PFS (SUV_{max} Cutoff at 5.25)

	Univariate Cox		Multivariate Cox	
PFS	HR	*P*	HR	*P*
SUV_{max}				
<5.25	Reference	—	Reference	—
≥5.25	2.11 (1.18–3.78)	0.01	1.92 (1.06–3.47)	0.03
WHO grades				
NET G1	Reference		Reference	
NET G2	1.25 (0.63–2.49)	0.52	1.22 (0.62–2.44)	0.56
NET G3	4.01 (1.68–9.54)	<0.01	3.94 (1.65–9.44)	<0.01
NEC	7.01 (2.65–18.50)	<0.001	5.84 (2.20–15.55)	<0.001

SUV_{max} cutoff optimized for prediction of OS was 5.25. Data in parentheses are 95% CIs.

TABLE 7
Uni- and Multivariate Cox Regression Analyses for OS (SUV_{max} Cutoff at 5.25)

	Univariate Cox		Multivariate Cox	
OS	HR	*P*	HR	*P*
SUV_{max}				
<5.25	Reference	—	Reference	—
≥5.25	6.95 (1.64–29.51)	0.01	5.45 (1.26–23.60)	0.02
WHO grades				
NET G1	Reference		Reference	
NET G2	1.84 (0.40–8.50)	0.44	1.78 (0.38–8.26)	0.46
NET G3	15.99 (3.26–78.50)	<0.01	15.67 (3.13–78.47)	<0.001
NEC	28.46 (5.62–144.24)	<0.001	20.23 (3.98–102.87)	<0.001

SUV_{max} cutoff optimized for prediction of OS was 5.25. Data in parentheses are 95% CIs.

gene expression analysis in patients with pulmonary NEN. Upregulation of fibrogenic genes, including ITGAV (the gene encoding integrin α_v), was related to poor differentiation and increased risk of metastases (*22*). However, conflicting data regarding the relation between poorer prognosis and integrin $\alpha_v\beta_3$ expression have been reported for immunohistochemical staining of gastric cancer (*23*) and non–small cell lung cancer (*24*).

Spurred by the upregulation of $\alpha_v\beta_3$ during angiogenesis, early phase clinical trials with the $\alpha_v\beta_3/\alpha_v\beta_5$-targeting ligand cilengitide were performed, showing modest effect on tumor growth (*25,26*). However, later phase II and phase III trials failed to meet expectations because of an unintended proangiogenic effect at lower concentrations while an antiangiogenetic effect was seen only at higher concentration (*27*). Recently, new promising pure $\alpha_v\beta_3$ ligands (TDI-4161 and TDI-3761) have been shown to circumvent the proangiogenetic effect previously seen with cilengitide (*28*), hence reinforcing the need for development of methods as companion diagnostics to assess in vivo the level of integrin $\alpha_v\beta_3$ expression for selection of patients for such targeted therapies.

Another possible avenue for integrin $\alpha_v\beta_3$-targeted treatments is PRRT. In patients with NEN, PRRT with ^{177}Lu-DOTATATE, exploiting somatostatin receptor overexpression, has become an integrated part of treatment (*29,30*). In 2 preclinical studies, the potential of extending the use of the RGD sequence by coupling it with a radionuclide for therapy has been examined. One combined $\alpha_v\beta_3$-targeting PRRT with immune checkpoint inhibitor programmed death ligand 1 (*31*) and the other $\alpha_v\beta_3$-targeting PRRT with temozolomide (*32*). Both demonstrated additional effect of the combined therapy. Further studies of coupling imaging and PRRT in the setting of integrin $\alpha_v\beta_3$ are needed. Concerns over physiologic uptake reported in RGD-based imaging have been raised regarding PRRT (*20*). However, compared with dosimetry data from somatostatin-based PET radiotracers ^{68}Ga-DOTATATE and ^{68}Ga-DOTATOC (*33*), we found similar kidney, liver, spleen, and intestinal absorbed doses in our phase I trial study assessing the dosimetry of ^{68}Ga-NODAGA-E[c(RGDyK)]$_2$ (*9*). Finally, a potential advantage of $\alpha_v\beta_3$-targeting PRRT over somatostatin receptor–targeting PRRT in NEN is that in particular in high-grade tumors, somatostatin receptor expression is low or absent and therefore somatostatin receptor PRRT cannot be used. In contrast, we found a high uptake of ^{68}Ga-NODAGA-E[c(RGDyK)]$_2$ also in high-grade tumors (91% of patients with NET G3/NEC).

In our study, included patients predominately had small intestinal or pancreatic primary tumors and nearly all had metastatic disease with liver involvement. Hence use of ^{68}Ga-NODAGA-E[c(RGDyK)]$_2$ PET/CT in other settings, for example, for assessment of newly diagnosed patients with localized disease, remains to be elucidated.

CONCLUSION

Tumor uptake of ^{68}Ga-NODAGA-E[c(RGDyK)]$_2$ was evident in patients both with low- and with high-grade NEN, although tumor uptake was more pronounced with increasing grade. High tumor uptake of ^{68}Ga-NODAGA-E[c(RGDyK)]$_2$ was associated with a poorer prognosis in patients with NEN, with a 2-fold higher risk of progression and 7-fold higher risk of death. Further studies are warranted to establish whether ^{68}Ga-NODAGA-E[c(RGDyK)]$_2$ PET/CT may become a tool for risk stratification and for identification of patients eligible for treatments targeting integrin $\alpha_v\beta_3$.

DISCLOSURE

This project received funding from the European Union's Horizon 2020 research and innovation program under grant agreements no. 670261 (ERC Advanced Grant) and 668532 (Click-It), the Lundbeck Foundation, the Novo Nordisk Foundation, the Innovation Fund Denmark, IPSEN Nordic, the Danish Cancer Society, Arvid Nilsson Foundation, the Neye Foundation, Novartis Health Care, the Research Foundation of Rigshospitalet, the Danish National Research Foundation (grant 126), the Research Council of the Capital Region of Denmark, the Danish Health Authority, the John and Birthe Meyer Foundation, the Research Council for Independent Research, and the Neuroendocrine Tumor Research Foundation. Andreas Kjaer is a Lundbeck Foundation Professor and is an inventor/holds intellectual property rights on a patent application: "^{68}Ga- and ^{64}Cu -NODAGA-E[c(RGDyK)]2 for use as pet tracers in the imaging of angiogenesis in humans" (WO2019091534A1). No other potential conflicts of interest relevant to this article exist.

ACKNOWLEDGEMENT

We are grateful to our dedicated colleagues at the Department of Clinical Physiology and Nuclear Medicine, Department of Endocrinology, and Department of Oncology at Rigshospitalet for assistance with patient recruitment, radiotracer production, and acquisition of PET/CT scans. We express our sincere gratitude to all the patients who participated in the study.

KEY POINTS

QUESTION: Is integrin $\alpha_v\beta_3$ expression assessed by PET evident in tumor lesions of patients with NENs and associated with prognosis?

PERTINENT FINDINGS: When ^{68}Ga-NODAGA-E[c(RGDyK)]$_2$ for integrin $\alpha_v\beta_3$ PET imaging was used, integrin $\alpha_v\beta_3$ was evident in tumor lesions of patients with both low- and high-grade tumors. High tumor uptake of ^{68}Ga-NODAGA-E[c(RGDyK)]$_2$ was associated with a poorer prognosis for both disease progression and death.

IMPLICATIONS FOR PATIENT CARE: Integrin $\alpha_v\beta_3$ is a prognostic marker and a potential treatment target in patients with NENs. ^{68}Ga-NODAGA-E[c(RGDyK)]$_2$ PET/CT may become a tool for risk stratification and for identification of patients eligible for treatments targeting integrin $\alpha_v\beta_3$.

REFERENCES

1. Dasari A, Shen C, Halperin D, et al. Trends in the incidence, prevalence, and survival outcomes in patients with neuroendocrine tumors in the United States. *JAMA Oncol.* 2017;3:1335–1342.
2. Digestive System Tumours. *WHO Classification of Tumours.* 5th ed. International Agency for Research on Cancer; 2019:16–19.
3. Carlsen EA, Johnbeck CB, Loft M, et al. Semiautomatic tumor delineation for evaluation of ^{64}Cu-DOTATATE PET/CT in patients with neuroendocrine neoplasms: prognostication based on lowest lesion uptake and total tumor volume. *J Nucl Med.* 2021;62:1564–1570.
4. Binderup T, Knigge U, Johnbeck CB, et al. ^{18}F-FDG PET is superior to WHO grading as a prognostic tool in neuroendocrine neoplasms and useful in guiding PRRT: a prospective 10-year follow-up study. *J Nucl Med.* 2021;62:808–815.
5. Ludwig BS, Kessler H, Kossatz S, Reuning U. RGD-binding integrins revisited: how recently discovered functions and novel synthetic ligands (re-)shape an ever-evolving field. *Cancers (Basel).* 2021;13:1711.
6. Nieberler M, Reuning U, Reichart F, et al. Exploring the role of RGD-recognizing integrins in cancer. *Cancers (Basel).* 2017;9:116.
7. Cives M, Pelle E, Quaresmini D, Rizzo FM, Tucci M, Silvestris F. The tumor microenvironment in neuroendocrine tumors: biology and therapeutic implications. *Neuroendocrinology.* 2019;109:83–99.
8. Oxboel J, Binderup T, Knigge U, Kjaer A. Quantitative gene-expression of the tumor angiogenesis markers vascular endothelial growth factor, integrin αV and integrin β3 in human neuroendocrine tumors. *Oncol Rep.* 2009;21:769–775.
9. Clausen MM, Carlsen EA, Christensen C, et al. First-in-human study of [^{68}Ga]Ga-NODAGA-E[c(RGDyK)]2 PET for integrin alphavbeta3 imaging in patients with breast cancer and neuroendocrine neoplasms: safety, dosimetry and tumor imaging ability. *Diagnostics (Basel).* 2022;12:851.
10. Oxboel J, Brandt-Larsen M, Schjoeth-Eskesen C, et al. Comparison of two new angiogenesis PET tracers ^{68}Ga-NODAGA-E[c(RGDyK)]2 and ^{64}Cu-NODAGA-E[c(RGDyK)]2; in vivo imaging studies in human xenograft tumors. *Nucl Med Biol.* 2014;41:259–267.
11. Knigge U, Capdevila J, Bartsch DK, et al. ENETS consensus recommendations for the standards of care in neuroendocrine neoplasms: follow-up and documentation. *Neuroendocrinology.* 2017;105:310–319.
12. Eisenhauer EA, Therasse P, Bogaerts J, et al. New response evaluation criteria in solid tumours: revised RECIST guideline (version 1.1). *Eur J Cancer.* 2009;45:228–247.
13. Budczies J, Klauschen F, Sinn BV, et al. Cutoff Finder: a comprehensive and straightforward web application enabling rapid biomarker cutoff optimization. *PLoS One.* 2012;7:e51862.
14. Liolios C, Sachpekidis C, Kolocouris A, Dimitrakopoulou-Strauss A, Bouziotis P. PET diagnostic molecules utilizing multimeric cyclic RGD peptide analogs for imaging integrin alphavbeta3 receptors. *Molecules.* 2021;26:1792.
15. Zheng Y, Wang H, Tan H, et al. Evaluation of lung cancer and neuroendocrine neoplasm in a single scan by targeting both somatostatin receptor and integrin αvβ3. *Clin Nucl Med.* 2019;44:687–694.
16. Dietz M, Kamani CH, Deshayes E, et al. Imaging angiogenesis in atherosclerosis in large arteries with ^{68}Ga-NODAGA-RGD PET/CT: relationship with clinical atherosclerotic cardiovascular disease. *EJNMMI Res.* 2021;11:71.
17. Wu J, Wang S, Zhang X, et al. ^{18}F-Alfatide II PET/CT for identification of breast cancer: a preliminary clinical study. *J Nucl Med.* 2018;59:1809–1816.
18. Zhu Z, Yin Y, Zheng K, et al. Evaluation of synovial angiogenesis in patients with rheumatoid arthritis using ^{68}Ga-PRGD2 PET/CT: a prospective proof-of-concept cohort study. *Ann Rheum Dis.* 2014;73:1269–1272.
19. Durante S, Dunet V, Gorostidi F, et al. Head and neck tumors angiogenesis imaging with ^{68}Ga-NODAGA-RGD in comparison to ^{18}F-FDG PET/CT: a pilot study. *EJNMMI Res.* 2020;10:47.
20. Steiger K, Quigley NG, Groll T, et al. There is a world beyond alphavbeta3-integrin: multimeric ligands for imaging of the integrin subtypes alphavbeta6, alphavbeta8, alphavbeta3, and alpha5beta1 by positron emission tomography. *EJNMMI Res.* 2021;11:106.
21. Mahmood N, Mihalcioiu C, Rabbani SA. Multifaceted role of the urokinase-type plasminogen activator (uPA) and its receptor (uPAR): diagnostic, prognostic, and therapeutic applications. *Front Oncol.* 2018;8:24.
22. Prieto TG, Machado-Rugolo J, Baldavira CM, et al. The fibrosis-targeted collagen/integrins gene profile predicts risk of metastasis in pulmonary neuroendocrine neoplasms. *Front Oncol.* 2021;11:706141.
23. Böger C, Warneke VS, Behrens HM, et al. Integrins alphavbeta3 and alphavbeta5 as prognostic, diagnostic, and therapeutic targets in gastric cancer. *Gastric Cancer.* 2015;18:784–795.
24. Böger C, Kalthoff H, Goodman SL, Behrens H-M, Röcken C. Integrins and their ligands are expressed in non-small cell lung cancer but not correlated with parameters of disease progression. *Virchows Arch.* 2014;464:69–78.
25. Nabors LB, Mikkelsen T, Hegi ME, et al. A safety run-in and randomized phase 2 study of cilengitide combined with chemoradiation for newly diagnosed glioblastoma (NABTT 0306). *Cancer.* 2012;118:5601–5607.
26. Reardon DA, Fink KL, Mikkelsen T, et al. Randomized phase II study of cilengitide, an integrin-targeting arginine-glycine-aspartic acid peptide, in recurrent glioblastoma multiforme. *J Clin Oncol.* 2008;26:5610–5617.
27. Stupp R, Hegi ME, Gorlia T, et al. Cilengitide combined with standard treatment for patients with newly diagnosed glioblastoma with methylated MGMT promoter (CENTRIC EORTC 26071-22072 study): a multicentre, randomised, open-label, phase 3 trial. *Lancet Oncol.* 2014;15:1100–1108.
28. Li J, Fukase Y, Shang Y, et al. Novel pure alphaVbeta3 integrin antagonists that do not induce receptor extension, prime the receptor, or enhance angiogenesis at low concentrations. *ACS Pharmacol Transl Sci.* 2019;2:387–401.
29. Janson ET, Knigge U, Dam G, et al. Nordic guidelines 2021 for diagnosis and treatment of gastroenteropancreatic neuroendocrine neoplasms. *Acta Oncol.* 2021;60:931–941.
30. Hope TA, Bodei L, Chan JA, et al. NANETS/SNMMI consensus statement on patient selection and appropriate use of ^{177}Lu-DOTATATE peptide receptor radionuclide therapy. *J Nucl Med.* 2020;61:222–227.
31. Chen H, Zhao L, Fu K, et al. Integrin alphavbeta3-targeted radionuclide therapy combined with immune checkpoint blockade immunotherapy synergistically enhances anti-tumor efficacy. *Theranostics.* 2019;9:7948–7960.
32. Lee SH, Choi JY, Jung JH, et al. Effect of peptide receptor radionuclide therapy in combination with temozolomide against tumor angiogenesis in a glioblastoma model. *Cancers (Basel).* 2021;13:5029.
33. Sandström M, Velikyan I, Garske-Román U, et al. Comparative biodistribution and radiation dosimetry of ^{68}Ga-DOTATOC and ^{68}Ga-DOTATATE in patients with neuroendocrine tumors. *J Nucl Med.* 2013;54:1755–1759.